Hindawi
Mathematical Problems in Engineering
Volume 2018, Article ID 1767645, 8 pages
https://doi.org/10.1155/2018/1767645

Research Article

Mixed Electrical Conditions on Interface Inclusion in a Piezoelectric Bimaterial under Antiplane Mechanical and Inplane Electric Loadings

A. Sheveleva[1] **V. Loboda**[2] **and A. Kryvoruchko**[2]

[1]*Department of Computational Mathematics, Oles Honchar Dnipro National University, Gagarin Av. 72, Dnipro 49010, Ukraine*
[2]*Department of Theoretical and Computational Mechanics, Oles Honchar Dnipro National University, Gagarin Av. 72, Dnipro, 49010, Ukraine*

Correspondence should be addressed to V. Loboda; loboda@dnu.dp.ua

Received 28 December 2017; Accepted 8 May 2018; Published 5 June 2018

Academic Editor: Marco Morandini

An absolutely rigid interface inclusion in a bimaterial piezoelectric space under the action of antiplane mechanical and in-plane electric loadings is analyzed. One zone of the inclusion is electrically insulated while the other part is electrically permeable. This problem is important for engineering application, but it has not been solved earlier in an analytical way. Presenting all electromechanical quantities via sectionally analytic vector functions, the combined Dirichlet-Riemann boundary value problem is formulated. An exact analytical solution of this problem is obtained. Closed form analytical expressions for electromechanical quantities at the interface are derived. Some of these values are also presented graphically along the corresponding parts of the material interface. Singular points of the shear strain and the electric displacement are found and the corresponding intensity factors are determined as well.

1. Introduction

Piezoelectric materials are used in many engineering applications. These materials are often integrated into sensors, transducers, and actuators, where they can be exposed to substantial mechanical and electrical loading. However, existing microdefects, particularly interface inclusions, can reduce their strength. Therefore, it is very important to study the behavior of piezoelectric ceramics with internal and especially interface defects subjected to the action of mechanical stresses and electrical fields.

Many important solutions have been obtained for inclusions in electrically passive materials. For example, the problem of rigid line inclusions in a homogeneous infinite matrix was studied in [1–6] and an interfacial inclusion between two dissimilar media was investigated in [7–9]. Rigid line inclusions in a piezoelectric medium were also actively studied. For instance, Liang et al. [10] and Chen [11] studied the in-plane and antiplane problems, respectively, of a homogeneous infinite piezoelectric medium with such inclusions.

Essential progress was made concerning the investigation of rigid inclusions at the interface of piezoelectric materials. Particularly the electroelastic analysis of a conducting rigid line inclusion at the interface of two bonded piezoelectric materials is considered in paper [12]. By combining the analytic function theory and the Stroh formalism the closed-form expressions for the field variables were found. In the paper [13] the generalized two-dimensional problem of a dielectric rigid line inclusion, at the interface between two dissimilar piezoelectric media subjected to piecewise uniform loads at infinity, is studied by means of the Stroh theory. The problem was reduced to a Hilbert problem, and then closed-form expressions were obtained. The special mixed boundary value problem in which a debonded conducting rigid line inclusion is embedded at the interface of two piezoelectric half planes is solved analytically in [14] by employing Stroh formalism. The model based on the assumption that all of the physical quantities, i.e., tractions, displacements, normal component of electric displacements, and electric potential, are discontinuous across the interface defect was used in this paper. The axisymmetric contact problem of a rigid inclusion embedded in the piezoelectric bimaterial frictionless interface subjected to simultaneous far-field compression and electric displacement is studied in [15]. An arc-shaped conducting rigid line inclusion located at the interface between a circular piezoelectric inhomogeneity and an unbounded piezoelectric matrix subjected to remote uniform antiplane shear stresses and in-plane electric fields is considered recently in [16].

It should be mentioned that all results concerning the rigid inclusions at the interface between piezoelectric materials are related to the cases of one-type electric conditions at the inclusion. However, in some cases important for engineering applications these conditions can be mixed, i.e., they can change from one part of the inclusion to another. The problem in such case becomes mathematically much more complicated; therefore, the associated analytical solutions are absent to the authors knowledge. Just such solution is suggested in the present paper for a certain case of mixed electrical conditions on the interface inclusion.

2. Basic Equations for a Piezoelectric Material under Out-of-Plane Mechanical Loading and In-Plane Electric Loading

For a piezoelectric material the relationship between the main electromechanical characteristics are defined by the relations (Parton and Kudryavtsev [17])

$$\begin{aligned}\sigma_{ij} &= c_{ijks}\varepsilon_{ks} - e_{sij}E_s,\\ D_i &= e_{iks}\varepsilon_{ks} + \alpha_{is}E_s,\end{aligned} \tag{1}$$

where σ_{ij}, ε_{ij} are the components of stress and strain tensor, D_i, E_i are the components of the electric induction and the electric field, c_{ijks}, e_{sij} are elastic and piezoelectric constants, and α_{is} are dielectric constants.

The equilibrium equations in the absence of body forces and free charges are

$$\begin{aligned}\sigma_{ij,j} &= 0,\\ D_{i,i} &= 0.\end{aligned} \tag{2}$$

The expressions for the deformation and electric field have the form

$$\begin{aligned}\varepsilon_{ij} &= \frac{1}{2}\left(u_{i,j} + u_{j,i}\right),\\ E_i &= -\varphi_{,i},\end{aligned} \tag{3}$$

where u_i are the components of the displacement vector and φ is the electric potential.

For the out-of-plane mechanical loading and in-plane electric loading assuming the material is transversely isotropic with the poling direction parallel to the x_3-axis, one has

$$\begin{aligned}u_1 &= u_2 = 0,\\ u_3 &= u_3\left(x_1, x_2\right),\\ \varphi &= \varphi\left(x_1, x_2\right).\end{aligned} \tag{4}$$

Then the constitutive relations take the form

$$\begin{Bmatrix}\sigma_{3i}\\ D_i\end{Bmatrix} = \mathbf{R}\begin{Bmatrix}u_{3,i}\\ \varphi_{,i}\end{Bmatrix}, \tag{5}$$

where $i = 1, 2$ and $\mathbf{R} = \left[\begin{smallmatrix}c_{44} & e_{15}\\ e_{15} & -\alpha_{11}\end{smallmatrix}\right]$.

Introducing the vectors

$$\begin{aligned}\mathbf{u} &= \left[u_3, \varphi\right]^T,\\ \mathbf{t} &= \left[\sigma_{32}, D_2\right]^T,\end{aligned} \tag{6}$$

one can write

$$\mathbf{t} = \mathbf{R}\mathbf{u}_{,2}. \tag{7}$$

The functions u_3 and φ satisfy the equations $\Delta u_3 = 0$, $\Delta\varphi = 0$; i.e., they are harmonic. Therefore, present them as real parts of some analytic functions

$$\mathbf{u} = 2\mathrm{Re}\boldsymbol{\Phi}(z) = \boldsymbol{\Phi}(z) + \overline{\boldsymbol{\Phi}}(\bar{z}), \tag{8}$$

where $\boldsymbol{\Phi}(z) = [\Phi_1(z), \Phi_2(z)]^T$ is an arbitrary analytic function of the complex variable $z = x_1 + ix_2$.

Substituting (8) into (7), one gets

$$\mathbf{t} = i\mathbf{R}\boldsymbol{\Phi}'(z) + \overline{i\mathbf{R}\boldsymbol{\Phi}'(z)}. \tag{9}$$

Using the designation $\mathbf{Q} = i\mathbf{R}$, we arrive to the equations

$$\mathbf{t} = \mathbf{Q}\boldsymbol{\Phi}'(z) + \overline{\mathbf{Q}}\,\overline{\boldsymbol{\Phi}}'(\bar{z}). \tag{10}$$

To achieve the purposes of this paper we have to transform further the presentations (8) and (10). Taking into account that

$$\mathbf{u}' = \boldsymbol{\Phi}'(z) + \overline{\boldsymbol{\Phi}}'(\bar{z}) \tag{11}$$

and introducing the vectors

$$\begin{aligned}\mathbf{v}' &= \left[\sigma_{32}, -E_1\right]^T,\\ \mathbf{P} &= \left[u_3', \mathrm{D}_2\right]^T,\end{aligned} \tag{12}$$

the following relations can be formulated

$$\mathbf{v}' = \mathbf{A}\boldsymbol{\Phi}'(z) + \overline{\mathbf{A}}\,\overline{\boldsymbol{\Phi}}'(\bar{z}), \tag{13}$$

$$\mathbf{P} = \mathbf{B}\boldsymbol{\Phi}'(z) + \overline{\mathbf{B}}\,\overline{\boldsymbol{\Phi}}'(\bar{z}), \tag{14}$$

where the matrixes $\mathbf{A}$ and $\mathbf{B}$ are the following:

$$\begin{aligned}\mathbf{A} &= \begin{bmatrix}Q_{11} & Q_{12}\\ 0 & 1\end{bmatrix},\\ \mathbf{B} &= \begin{bmatrix}1 & 0\\ Q_{21} & Q_{22}\end{bmatrix}.\end{aligned} \tag{15}$$

3. Bimaterial Case

Suppose that the plane (x_1, x_2) is composed of two half-planes $x_2 > 0$ and $x_2 < 0$. The presentations (13) and (14) can be written for regions $x_2 > 0$ and $x_2 < 0$ in the form

$$\mathbf{v}^{(m)} = \mathbf{A}^{(m)}\mathbf{\Phi}^{(m)}(z) + \overline{\mathbf{A}}^{(m)}\overline{\mathbf{\Phi}}^{(m)}(\overline{z}),$$
$$\mathbf{P}^{(m)} = \mathbf{B}^{(m)}\mathbf{\Phi}'^{(m)}(z) + \overline{\mathbf{B}}^{(m)}\overline{\mathbf{\Phi}}'^{(m)}(\overline{z}), \quad (16)$$

where $m = 1$ for the region 1 and $m = 2$ for the region 2; $\mathbf{A}^{(m)}$ and $\mathbf{B}^{(m)}$ are the matrices $\mathbf{A}$ and $\mathbf{B}$ for the regions 1 and 2, respectively; $\mathbf{\Phi}^{(m)}(z)$ are arbitrary vector functions, analytic in the regions 1 and 2, respectively.

Next we require that the equality $\mathbf{P}^{(1)} = \mathbf{P}^{(2)}$ holds true on the entire axis x_1.Then it follows from (16)

$$\mathbf{B}^{(1)}\mathbf{\Phi}'^{(1)}(x_1 + i0) + \overline{\mathbf{B}}^{(1)}\overline{\mathbf{\Phi}}'^{(1)}(x_1 - i0)$$
$$= \mathbf{B}^{(2)}\mathbf{\Phi}'^{(2)}(x_1 - i0) + \overline{\mathbf{B}}^{(2)}\overline{\mathbf{\Phi}}'^{(2)}(x_1 + i0). \quad (17)$$

Here $F(x_1 \pm i0)$ designates the limit value of a function $F(z)$ at $y \to 0$ from above or below the x_1-axis, respectively. Equation (17) can be written as

$$\mathbf{B}^{(1)}\mathbf{\Phi}'^{(1)}(x_1 + i0) - \overline{\mathbf{B}}^{(2)}\overline{\mathbf{\Phi}}'^{(2)}(x_1 + i0)$$
$$= \mathbf{B}^{(2)}\mathbf{\Phi}'^{(2)}(x_1 - i0) - \overline{\mathbf{B}}^{(1)}\overline{\mathbf{\Phi}}'^{(1)}(x_1 - i0). \quad (18)$$

The left and right sides of the last equation can be considered as the boundary values of the functions

$$\mathbf{B}^{(1)}\mathbf{\Phi}'^{(1)}(z) - \overline{\mathbf{B}}^{(2)}\overline{\mathbf{\Phi}}'^{(2)}(z),$$
$$\mathbf{B}^{(2)}\mathbf{\Phi}'^{(2)}(z) - \overline{\mathbf{B}}^{(1)}\overline{\mathbf{\Phi}}'^{(1)}(z), \quad (19)$$

which are analytic in the upper and lower planes, respectively. But it means that there is a function $\mathbf{M}(z)$, which is equal to the mentioned functions in each half-plane and is analytic in the entire plane.

Assuming that $\mathbf{M}(z)|_{z\to\infty} \to 0$, on the basis of the Liouville theorem we find that each of the functions in (19) is equal to 0 for any z from the corresponding half-plane. Hence, we obtain

$$\overline{\mathbf{\Phi}}'^{(2)}(\mathrm{z}) = \left(\overline{\mathbf{B}}^{(2)}\right)^{-1}\mathbf{B}^{(1)}\mathbf{\Phi}'^{(1)}(\mathrm{z}) \quad \text{for } x_2 > 0,$$
$$\overline{\mathbf{\Phi}}'^{(1)}(\mathrm{z}) = \left(\overline{\mathbf{B}}^{(1)}\right)^{-1}\mathbf{B}^{(2)}\mathbf{\Phi}'^{(2)}(\mathrm{z}) \quad \text{for } x_2 < 0. \quad (20)$$

Further, we find the jump of the vector function

$$\left\langle \mathbf{v}'(x_1)\right\rangle = \mathbf{v}'^{(1)}(x_1 + i0) - \mathbf{v}'^{(2)}(x_1 - i0), \quad (21)$$

when passing through the interface. Determining from the first formula (16)

$$\mathbf{v}'^{(m)}(z) = \mathbf{A}^{(m)}\mathbf{\Phi}'^{(m)}(z) + \overline{\mathbf{A}}^{(m)}\overline{\mathbf{\Phi}}'^{(m)}(\overline{z}) \quad (22)$$

or

$$\mathbf{v}'^{(m)}(x_1 \pm i0) = \mathbf{A}^{(m)}\mathbf{\Phi}'^{(m)}(x_1 \pm i0)$$
$$+ \overline{\mathbf{A}}^{(m)}\overline{\mathbf{\Phi}}'^{(m)}(x_1 \mp i0), \quad (23)$$

and substituting in (21), one gets

$$\left\langle \mathbf{v}'(x_1)\right\rangle = \mathbf{A}^{(1)}\mathbf{\Phi}'^{(1)}(x_1 + i0) + \overline{\mathbf{A}}^{(1)}\overline{\mathbf{\Phi}}'^{(1)}(x_1 - i0)$$
$$- \mathbf{A}^{(2)}\mathbf{\Phi}'^{(2)}(x_1 - i0) \quad (24)$$
$$- \overline{\mathbf{A}}^{(2)}\overline{\mathbf{\Phi}}'^{(2)}(x_1 + i0).$$

Finding further $\mathbf{\Phi}'^{(2)}(x_1 - i0) = (\mathbf{B}^{(2)})^{-1}\overline{\mathbf{B}}^{(1)}\overline{\mathbf{\Phi}}'^{(1)}(x_1 - i0)$ from second equation of (20) and substituting this expression together with the first equation of (20) at $x_2 \to +0$ in the latest formula lead to

$$\left\langle \mathbf{v}'(x_1)\right\rangle = \mathbf{D}\mathbf{\Phi}'^{(1)}(x_1 + i0) + \overline{\mathbf{D}}\,\overline{\mathbf{\Phi}}'^{(1)}(x_1 - i0), \quad (25)$$

where $\mathbf{D} = \mathbf{A}^{(1)} - \overline{\mathbf{A}}^{(2)}(\overline{\mathbf{B}}^{(2)})^{-1}\mathbf{B}^{(1)}$. Introducing a new vector function

$$\mathbf{W}(z) = \begin{cases} \mathbf{D}\mathbf{\Phi}'^{(1)}(z), & x_2 > 0, \\ -\overline{\mathbf{D}}\,\overline{\mathbf{\Phi}}'^{(1)}(z), & x_2 < 0, \end{cases} \quad (26)$$

the last relation can be written as

$$\left\langle \mathbf{v}'(x_1)\right\rangle = \mathbf{W}^{+}(x_1) - \mathbf{W}^{-}(x_1). \quad (27)$$

From the second relations (16) we have

$$\mathbf{P}^{(1)}(x_1, 0) = \mathbf{B}^{(1)}\mathbf{\Phi}'^{(1)}(x_1 + i0)$$
$$+ \overline{\mathbf{B}}^{(1)}\overline{\mathbf{\Phi}}'^{(1)}(x_1 - i0). \quad (28)$$

Taking into account that on the base of (26)

$$\mathbf{\Phi}'^{(1)}(x_1 + i0) = \mathbf{D}^{-1}\mathbf{W}(x_1 + i0),$$
$$\overline{\mathbf{\Phi}}'^{(1)}(x_1 - i0) = -\left(\overline{\mathbf{D}}^{-1}\right)^{-1}\mathbf{W}(x_1 - i0), \quad (29)$$

and substituting these relations into (28), leads to

$$\mathbf{P}^{(1)}(x_1, 0) = \mathbf{S}\mathbf{W}^{+}(x_1) - \overline{\mathbf{S}}\mathbf{W}^{-}(x_1), \quad (30)$$

where $\mathbf{S} = \mathbf{B}^{(1)}\mathbf{D}^{-1}$. Simple calculations show that

$$\mathbf{S} = \left[\mathbf{A}^{(1)}\left(\mathbf{B}^{(1)}\right)^{-1} - \overline{\mathbf{A}}^{(2)}\left(\overline{\mathbf{B}}^{(2)}\right)^{-1}\right]^{-1}. \quad (31)$$

Representations (27) and (30) are very convenient for solving of antiplane problems for bimaterials with cracks and inclusions at the interface.

It is found out that for the considered class of piezoelectric materials the matrix $\mathbf{S}$ has the following structure:

$$\mathbf{S} = \begin{bmatrix} is_{11} & s_{12} \\ s_{21} & is_{22} \end{bmatrix}, \quad (32)$$

where all s_{kl} $(k, l = 1, 2)$ are real.

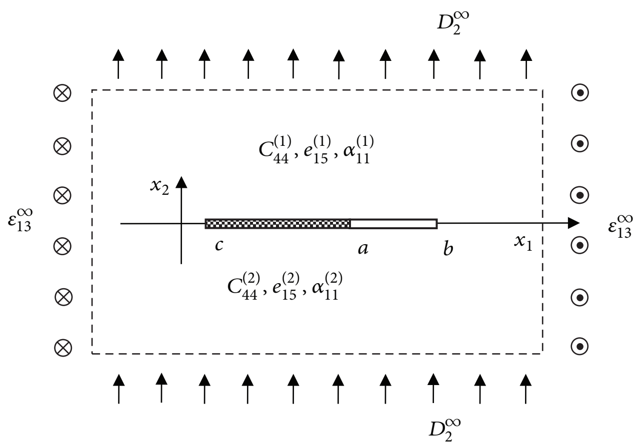

FIGURE 1: An absolutely rigid inclusion at the interface of two piezoelectric materials with electrically insulated part (c, a) and electrically permeable part (a, b).

4. Formulation of the Problem for an Absolutely Rigid Inclusion with Mixed Electrical Condition at the Face

Consider an absolutely rigid thin inclusion $c \le x_1 \le b$ at the interface $x_2 = 0$. It is assumed that this inclusion is electrically insulated for $c \le x_1 \le a$ and is electrically permeable at $a < x_1 < b$ $(a < b)$. Such situation can take place, e.g., for a rigid electrically permeable interface layer having a part covered by electrical insulator (Figure 1).

Then the boundary conditions at the interface are of the form

$$\varepsilon_{13}^{(1)} = \varepsilon_{13}^{(2)} = 0,$$
$$D_2^{(1)} = D_2^{(2)} = 0 \quad (33)$$
$$\text{for } c < x_1 < a,$$

$$\varepsilon_{13}^{(1)} = \varepsilon_{13}^{(2)} = 0,$$
$$\langle E_1 \rangle = 0$$
$$\langle D_2 \rangle = 0 \quad (34)$$
$$\text{for } a < x_1 < b,$$

$$\langle \sigma_{23} \rangle = 0,$$
$$\langle D_2 \rangle = 0,$$
$$\langle \varepsilon_{31} \rangle = 0, \quad (35)$$
$$\langle E_1 \rangle = 0$$
$$\text{for } x_1 \notin (c, b).$$

We also assume that a vector $\mathbf{P}^{\infty} = [\varepsilon_{13}^{\infty}, D_2^{\infty}]^T$ is prescribed at infinity.

Consider (30) in the following expanded form:

$$\varepsilon_{13}^{(1)}(x_1, 0) = is_{11}W_1^+(x_1) + s_{12}W_2^+(x_1) + is_{11}W_1^-(x_1) - s_{12}W_2^-(x_1),$$
$$D_2^{(1)}(x_1, 0) = s_{21}W_1^+(x_1) + is_{22}W_2^+(x_1) - s_{21}W_1^-(x_1) + is_{22}W_2^-(x_1), \quad (36)$$

in which (32) was taken into account. Combining (36) one arrives at the presentations

$$\varepsilon_{13}^{(1)}(x_1, 0) - im_j D_2^{(1)}(x_1, 0) = t_j \left[F_j^+(x_1) + \gamma_j F_j^-(x_1)\right], \quad (37)$$

where

$$F_j(z) = W_2(z) + is_j W_1(z), \quad (38)$$

and $t_j = s_{12} - m_j s_{22}$, $\gamma_j = -(s_{12} + m_j s_{22})/t_j$, $s_j = (s_{11} + m_j s_{21})/t_j$, $m_{1,2} = \mp\sqrt{-s_{11}s_{12}/s_{21}s_{22}}$.

It follows from the last equations that $s_{1,2} = -m_{1,2}$, $\gamma_2 = 1/\gamma_1$, and the values $m_{1,2}$ are real.

Because according to (38) $F_j^+(x_1) - F_j^-(x_1) = W_2^+(x_1) - W_2^-(x_1) + is_j[W_1^+(x_1) - W_1^-(x_1)]$, then with use of (27) one gets

$$\langle -E_1(x_1, 0)\rangle + is_j \langle \sigma_{23}(x_1, 0)\rangle = F_j^+(x_1) - F_j^-(x_1). \quad (39)$$

It is sufficient to apply relations (37) and (39) in the following analysis only for $j = 1$; therefore, assuming $j = 1$, (37) and (39) can be presented in the form

$$\varepsilon_{13}^{(1)}(x_1, 0) - im_1 D_2^{(1)}(x_1, 0) = t_1 \left[F_1^+(x_1) + \gamma_1 F_1^-(x_1)\right], \quad (40)$$

$$\langle -E_1(x_1, 0)\rangle + is_1 \langle \sigma_{23}(x_1, 0)\rangle = F_1^+(x_1) - F_1^-(x_1), \quad (41)$$

where $m_1 = -\sqrt{-s_{11}s_{12}/s_{21}s_{22}}$, $s_1 = -m_1$.

Taking into account that for $x_1 \notin (c, b)$ the relationships $F_1^+(x_1) = F_1^-(x_1) = F_1(x_1)$ are valid, it follows from (40) that

$$(1 + \gamma_1) t_1 F_1(x_1) = \varepsilon_{13}^{(1)}(x_1, 0) - im_1 D_2^{(1)}(x_1, 0) \quad \text{for } x_1 \longrightarrow \infty. \quad (42)$$

Using the fact that the function $F_1(z)$ is analytic in the whole plane cut along (c, b) and applying the conditions at infinity, one gets from the last equation

$$F_1(z)\big|_{z\to\infty} = \tilde{\varepsilon}_{13} - i\tilde{D}_2, \quad (43)$$

where

$$\tilde{\varepsilon}_{13} = \frac{\varepsilon_{13}^{\infty}}{r_1},$$
$$\tilde{D}_2 = \frac{m_1 D_2^{\infty}}{r_1}, \quad (44)$$
$$r_1 = (1 + \gamma_1) t_1.$$

5. Solution of the Problem

Consider now the problem formulated by the interface conditions (33)–(35) and illustrated by Figure 1. Relations (27) and (30) and, consequently, (40) and (41) ensure satisfying equation $\mathbf{P}^{(1)}(x_1, 0) = \mathbf{P}^{(2)}(x_1, 0)$ for the whole interface and, accordingly, satisfying the second and third interface conditions (35). Further satisfaction of first and forth conditions (35) provides the analyticity of the function $F_1(z)$ for the whole plane with a cut along the segment (c, b) of the interface. Satisfying the remaining boundary conditions (33) and (34) with use of (40) and (41), one gets the following equations:

$$\begin{aligned} &F_1^+(x_1) + \gamma_1 F_1^-(x_1) = 0 \quad \text{for } c < x_1 < a, \\ &\operatorname{Re}\left[F_1^+(x_1) + \gamma_1 F_1^-(x_1)\right] = 0, \\ &\operatorname{Re}\left[F_1^+(x_1) - F_1^-(x_1)\right] = 0 \\ &\qquad \text{for } a < x_1 < b. \end{aligned} \tag{45}$$

The last two relations lead to the equation

$$\operatorname{Re}F_1^{\pm}(x_1) = 0 \quad \text{for } a < x_1 < b. \tag{46}$$

Introducing further the substitution

$$F_1(z) = i\Phi_1(z), \tag{47}$$

system (34) and (35) can be written in the form

$$\Phi_1^+(x_1) + \gamma_1 \Phi_1^-(x_1) = 0 \quad \text{for } c < x_1 < a, \tag{48}$$

$$\operatorname{Im}\Phi_1^{\pm}(x_1) = 0 \quad \text{for } a < x_1 < b. \tag{49}$$

Taking into account that the function $\Phi_1(z)$ is analytic outside the segment $[c, b]$ and using the prescribed values of the stress and the electric fields at infinity, one gets, from (43) and (44), the following condition for $\Phi_1(z)$ at infinity

$$\Phi_1(z)\big|_{z\to\infty} = E_1^* - i\sigma_{32}^*, \tag{50}$$

where $E_1^* = -\widetilde{D}_2$, $\sigma_{32}^* = \widetilde{\varepsilon}_{13}$, $r_1 = t_1(1+\gamma_1)$.

Relations (48) and (49) present the combined Dirichlet-Riemann boundary value problem. The solution of such problem concerning a rigid stamp was found by Nahnein and Nuller [18] and, concerning an in-plane interface crack, it was developed by Loboda [19] and Kozinov et al. [20]. Using these results, an exact solution of problem (37) and (38) is the following:

$$\Phi_1(z) = P(z) X_1(z) + Q(z) X_2(z), \tag{51}$$

where

$$\begin{aligned} P(z) &= C_1 z + C_2, \\ Q(z) &= D_1 z + D_2, \\ X_1(z) &= \frac{ie^{i\phi(z)}}{\sqrt{(z-c)(z-b)}}, \\ X_2(z) &= \frac{e^{i\phi(z)}}{\sqrt{(z-c)(z-a)}}, \\ \varphi(z) &= 2\varepsilon \ln \frac{\sqrt{(b-a)(z-c)}}{\sqrt{l(z-a)} + \sqrt{(a-c)(z-b)}}, \\ \varepsilon &= \frac{1}{2\pi}\ln\gamma_1, \\ l &= b - c, \\ C_1 &= -\sigma_{32}^*\cos\beta - E_1^*\sin\beta, \\ D_1 &= E_1^*\cos\beta - \sigma_{32}^*\sin\beta, \\ C_2 &= -\frac{c+b}{2}C_1 - \beta_1 D_1, \\ D_2 &= \beta_1 C_1 - \frac{c+a}{2}D_1, \\ \beta &= \varepsilon\ln\frac{1-\sqrt{1-\lambda}}{1+\sqrt{1-\lambda}}, \\ \beta_1 &= \varepsilon\sqrt{(a-c)(b-c)}, \\ \lambda &= \frac{b-a}{l}. \end{aligned} \tag{52}$$

This solution satisfies the condition at infinity (50) and the equation $\int_c^b [F_1^+(x_1) - F_1^-(x_1)]dx_1 = 0$ (Knysh et al. [21]). The last equation is obtained using (41) from the conditions of the electric potential uniqueness for overcoming the inclusion and the requirement of its equilibrium.

Using solution (51) together with formula (40), one gets

$$\begin{aligned} m_1 D_2^{(1)}(x_1,0) + i\varepsilon_{13}^{(1)}(x_1,0) = &-\left[\frac{Q(x_1)}{\sqrt{x_1-a}}\right. \\ &\left.+\frac{iP(x_1)}{\sqrt{x_1-b}}\right]\frac{r_1\exp\left[i\varphi(x_1)\right]}{\sqrt{x_1-c}} \quad \text{for } x_1 > b, \end{aligned} \tag{53}$$

$$\begin{aligned} &m_1 D_2^{(1)}(x_1,0) \\ &= -\frac{t_1 P(x_1)}{\sqrt{(x_1-c)(b-x_1)}}\left[(1-\gamma_1)\cosh\varphi_0(x_1)\right. \\ &\quad\left.+(1+\gamma_1)\sinh\varphi_0(x_1)\right] \\ &\quad+-\frac{t_1 Q(x_1)}{\sqrt{(x_1-c)(x_1-a)}}\left[(1+\gamma_1)\cosh\varphi_0(x_1)\right. \\ &\quad\left.+(1-\gamma_1)\sinh\varphi_0(x_1)\right] \quad \text{for } a < x_1 < b, \end{aligned} \tag{54}$$

where $\varphi_0(x_1) = 2\varepsilon\tan^{-1}\sqrt{(a-c)(b-x_1)/((b-c)(x_1-a))}$.

Substituting solution (51) into (41) gives the following formulas:

$$s_1 \langle \sigma_{23}(x_1,0)\rangle + i\langle E_1(x_1,0)\rangle = 2\sqrt{\alpha}\left[\frac{P(x_1)}{\sqrt{b-x_1}} - i\frac{Q(x_1)}{\sqrt{a-x_1}}\right]\frac{\exp[i\varphi^*(x_1)]}{\sqrt{x_1-c}} \quad \text{for } c < x_1 < a, \tag{55}$$

$$\langle \sigma_{23}(x_1,0)\rangle = \frac{2}{s_1\sqrt{x_1-c}}\left[\frac{P(x_1)}{\sqrt{b-x_1}}\cosh\varphi_0(x_1) + \frac{Q(x_1)}{\sqrt{x_1-a}}\sinh\varphi_0(x_1)\right] \quad \text{for } a < x_1 < b, \tag{56}$$

where $\varphi^*(x_1) = 2\varepsilon\ln(\sqrt{(b-a)(x_1-c)}/(\sqrt{l(a-x_1)} + \sqrt{(a-c)(b-x_1)}))$, $\alpha = (\gamma_1+1)^2/(4\gamma_1)$.

It is very important that the obtained solution is not oscillating in this case at the right crack tip and, therefore, commonly used intensity factors can be introduced. Thus, we introduce further the following mechanical strain and electrical displacement intensity factors (IFs):

$$K_D = \lim_{x_1\to a+0}\sqrt{2\pi(x_1-a)}D_2^{(1)}(x_1,0),$$
$$K_\varepsilon = \lim_{x_1\to b+0}\sqrt{2\pi(x_1-b)}\varepsilon_{13}^{(1)}(x_1,0). \tag{57}$$

Using (54) and taking into account that $\varphi_0(a) = \ln\sqrt{\gamma_1}$, one can find

$$K_D = \frac{r_1 Q(a)}{m_1\sqrt{a-c}}\sqrt{\frac{2\pi}{\alpha}}. \tag{58}$$

The intensity factor K_ε can be found from formula (53) and can be written in the form

$$K_\varepsilon = r_1\sqrt{\frac{2\pi}{l}}P(b). \tag{59}$$

Substituting the expressions for $P(b)$ and $Q(a)$ one gets

$$K_D = \frac{1}{m_1}\sqrt{\frac{\pi l}{2\alpha}}\left[\sqrt{1-\lambda}\left(\varepsilon_{13}^{\infty}\cos\beta - m_1D_2^{\infty}\sin\beta\right) - 2\varepsilon\left(\varepsilon_{13}^{\infty}\sin\beta + m_1D_2^{\infty}\cos\beta\right)\right], \tag{60}$$

$$K_\varepsilon = \sqrt{\frac{\pi l}{2}}\left[\left(\varepsilon_{13}^{\infty}\sin\beta + m_1D_2^{\infty}\cos\beta\right) + 2\varepsilon\sqrt{1-\lambda}\left(\varepsilon_{13}^{\infty}\cos\beta - m_1D_2^{\infty}\sin\beta\right)\right]. \tag{61}$$

Use of (55) for $x_1 \to a-0$ permits obtaining the following expressions of $\langle\sigma_{23}(x_1,0)\rangle$ via the stress intensity factor K_ε:

$$\langle \sigma_{23}(x_1,0)\rangle = -\frac{2\alpha}{r_1 s_1}\frac{K_\varepsilon}{\sqrt{2\pi(a-x_1)}} \quad \text{for } x_1 \longrightarrow a-0. \tag{62}$$

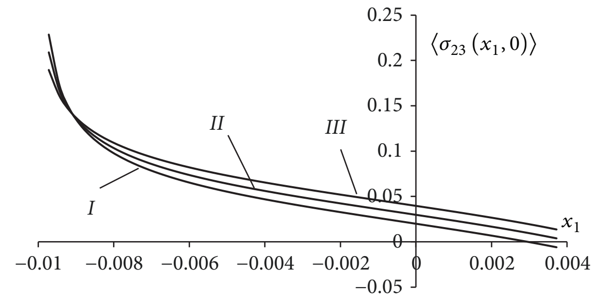

FIGURE 2: The shear stress $\langle\sigma_{23}(x_1,0)\rangle$ jump distribution over the insulated region of the inclusion for different values of $\varepsilon_{13}^{\infty}$.

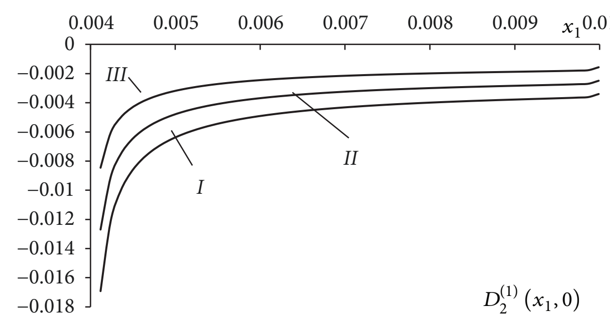

FIGURE 3: The electric displacement $D_2^{(1)}(x_1,0)$ for $x_1 \in (a,b)$.

6. Numerical Illustration

The results for the shear stress jump $\langle\sigma_{23}(x_1,0)\rangle$ for $c = -10$ mm, $b = 10$ mm, $D_2^{\infty} = 0.005\,\mathrm{C/m^2}$, and different values of $\varepsilon_{13}^{\infty}$ are shown in Figure 2. Lines I, II, and III in this figure correspond to $\varepsilon_{13}^{\infty} = 0.0001, 0.00015, 0.0002$, respectively. The results for the electric displacement $D_2^{(1)}(x_1,0)$ for $x_1 \in (a,b)$ and $x_1 > b$ are shown in Figures 3 and 4, respectively. The variation of the strain $\varepsilon_{13}^{(1)}(x_1,0)$ on the inclusion continuation is shown in Figure 5. The same values of $\varepsilon_{13}^{\infty}$ as in Figure 2 were chosen in Figures 3–5. The materials with the characteristics $c_{44}^{(1)} = 43{,}7\cdot10^9$ Pa, $e_{15}^{(1)} = 17\,\mathrm{C/m^2}$, $\alpha_{11}^{(1)} = 15{,}1\cdot10^{-9}$ C/(V·m), $c_{44}^{(2)} = 42{,}47\cdot10^9$ Pa, $e_{15}^{(2)} = -0{,}48\,\mathrm{C/m^2}$, and $\alpha_{11}^{(2)} = 0{,}0757\cdot10^{-9}$ C/(V·m) [22] were used for these calculations.

It can be seen from the results in Figure 2 that the stress jump is sufficiently small at the point a, but it grows with tending x_1 to the left tip of the inclusion. On the other hand the electric displacement $D_2^{(1)}(x_1,0)$ essentially grows at the right neighborhood of the point a (Figure 3) and keeps moderate values at the left vicinity of the right crack tip. It is interesting to note that $D_2^{(1)}(x_1,0)$ remains limited at the right vicinity of the point b and, moreover, it modestly decreases at a distance from this point (Figure 4). At the same time as it follows from Figure 5 the shear deformation $\varepsilon_{13}^{(1)}(x_1,0)$ is singular at the right neighborhood of the point b. Therefore, it grows very fast for x_1 tending to this point and it promptly decreases a distance from it.

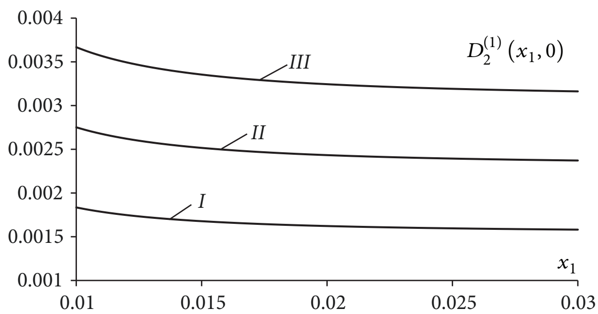

FIGURE 4: The electric displacement $D_2^{(1)}(x_1, 0)$ for $x_1 > b$.

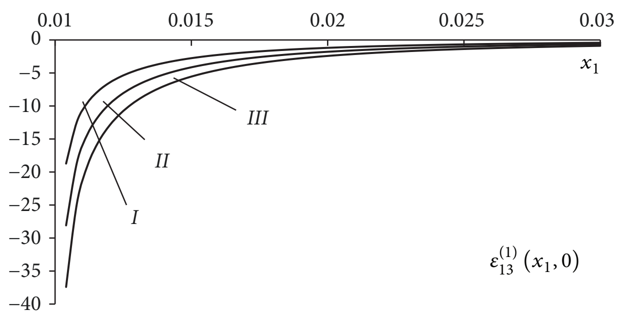

FIGURE 5: The variation of the strain $\varepsilon_{13}^{(1)}(x_1, 0)$ on the inclusion continuation.

7. Conclusion

A rigid inclusion between two semi-infinite piezoelectric spaces with electrically insulated and electrically permeable parts of the crack faces under the action of antiplane mechanical and in-plane electric loadings has been analyzed. This problem is important for engineering application, because the presence of inclusions disturbs the field variables in the matrixes and as a result affects the load-carrying capacity of engineering structure. Although such situation can take place for any engineering device containing piezoelectric element, it has not been investigated earlier in an analytical way to the authors' knowledge. Firstly the electromechanical quantities are presented by using of sectionally analytic vector functions. A combined Dirichlet-Riemann boundary value problem (48) and (49) is formulated and its exact analytical solution is derived. Analytical expressions (53)–(56) for the main electromechanical characteristics along the interface are presented in a closed form. Singular points of these values and the stress and electric intensity factors are determined. The variation of the shear stress jump $\langle\sigma_{23}(x_1, 0)\rangle$, electric displacement $D_2^{(1)}(x_1, 0)$, and the strain $\varepsilon_{13}^{(1)}(x_1, 0)$ along different sections of the inclusion and its continuation are presented in a graphical form for certain positions of the point a dividing the electrically insulated and electrically permeable zones of the inclusion.

Conflicts of Interest

The authors declare that there are no conflicts of interest regarding the publication of this paper.

References

[1] Z. Y. Wang, H. T. Zhang, and Y. T. Chou, "Characteristics of the elastic field of a rigid line inhomogeneity," *Journal of Applied Mechanics*, vol. 52, no. 4, pp. 818–822, 1985.

[2] Z. Y. Wang, H. T. Zhang, and Y. T. Chou, "Stress singularity at the tip of a rigid line inhomogeneity under antiplane shear loading," *Journal of Applied Mechanics*, vol. 53, no. 2, pp. 459–461, 1986.

[3] R. Ballarini, "An integral equation approach for rigid line inhomogeneity problems," *International Journal of Fracture*, vol. 33, no. 2, pp. R23–R26, 1987.

[4] Q. Li and T. C. Ting, "Line Inclusions in Anisotropic Elastic Solids," *Journal of Applied Mechanics*, vol. 56, no. 3, p. 556, 1989.

[5] Chen Yi-Heng and H.-G. Hahn, "The stress singularity coefficient at a finite rigid flat inclusion in an orthotropic plane elastic body," *Engineering Fracture Mechanics*, vol. 44, no. 3, pp. 359–362, 1993.

[6] H. Itou, A. M. Khludnev, E. M. Rudoy, and A. Tani, "Asymptotic behaviour at a tip of a rigid line inclusion in linearized elasticity," *ZAMM. Zeitschrift für Angewandte Mathematik und Mechanik. Journal of Applied Mathematics and Mechanics*, vol. 92, no. 9, pp. 716–730, 2012.

[7] R. Ballarini, "A rigid line inclusion at a bimaterial interface," *Engineering Fracture Mechanics*, vol. 37, no. 1, pp. 1–5, 1990.

[8] K.-C. Wu, "Line inclusions at anisotropic bimaterial interface," *Mechanics of Materials*, vol. 10, no. 3, pp. 173–182, 1990.

[9] A. Asundi and W. Deeg, "Rigid inclusions on the interface between two bonded anisotropic media," *Journal of the Mechanics and Physics of Solids*, vol. 13, pp. 1045–1058, 1995.

[10] J. Liang, J. Han, and S. Du, "Rigid line inclusions and cracks in anisotropic piezoelectric solids," *Mechanics Research Communications*, vol. 22, no. 1, pp. 43–49, 1995.

[11] S. Weichen, "Rigid line inclusions under anti-plane deformation and in-plane electric field in piezoelectric materials," *Engineering Fracture Mechanics*, vol. 56, no. 2, pp. 265–274, 1997.

[12] W. Deng and S. A. Meguid, "Analysis of conducting rigid inclusion at the interface of two dissimilar piezoelectric materials," *Journal of Applied Mechanics*, vol. 65, no. 1, pp. 76–84, 1998.

[13] G. Cun-fa and F. Wei-xun, "An interface inclusion between two dissimilar piezoelectric materials," *Applied Mathematics and Mechanics-English Edition*, vol. 22, no. 1, pp. 96–104, 2001.

[14] X. Wang and Y.-P. Shen, "Exact solution for mixed boundary value problems at anisotropic piezoelectric bimaterial interface and unification of various interface defects," *International Journal of Solids and Structures*, vol. 39, no. 6, pp. 1591–1619, 2002.

[15] M. Eskandari, S. S. Moeini-Ardakani, and H. M. Shodja, "Axisymmetric contact of a rigid inclusion embedded at the interface of a piezoelectric bimaterial," *The Quarterly Journal of Mechanics and Applied Mathematics*, vol. 62, no. 3, pp. 281–295, 2009.

[16] X. Wang and P. Schiavone, "Debonded arc-shaped interface conducting rigid line inclusions in piezoelectric composites," *Comptes Rendus (Doklady) de l'Academie des Sciences de l'URSS*, vol. 345, no. 10, pp. 724–731, 2017.

[17] V. Parton and B. Kudryavtsev, *Electromagnetoelasticity*, Gordon and Breach Science Publishers, New York, NY, USA, 1988.

[18] E. L. Nakhmein and B. M. Nuller, "Contact between an elastic half-plane and a partly separated stamp," *Journal of Applied Mathematics and Mechanics*, vol. 50, no. 4, pp. 507–515, 1986.

[19] V. V. Loboda, "The quasi-invariant in the theory of interface cracks," *Engineering Fracture Mechanics*, vol. 44, no. 4, pp. 573–580, 1993.

[20] S. Kozinov, V. Loboda, and Y. Lapusta, "Periodic set of limited electrically permeable interface cracks with contact zones," *Mechanics Research Communications*, vol. 48, pp. 32–41, 2013.

[21] P. Knysh, V. Loboda, F. Labesse-Jied, and Y. Lapusta, "An electrically charged crack in a piezoelectric material under remote electromechanical loading," *International Journal of Fracture*, vol. 175, no. 1, pp. 87–94, 2012.

[22] R. Li and G. A. Kardomateas, "The mode III interface crack in piezo-electro-magneto-elastic dissimilar bimaterials," *Journal of Applied Mechanics*, vol. 73, no. 2, pp. 220–227, 2006.